



e-ISSN: 2785-924X

https://jsst.uitm.edu.my/index.php/jsst

Journal of Smart Science and **Technology**

Journal of Smart Science and Technology 5(2) 2025, 36-62

Optimisation of a Geothermal Reservoir: A Case Study for Parryland Field

Melissa Ragoobar^{1*}, David Alexander¹ and Edward Bahaw¹

¹Energy Systems Engineering Unit, University of Trinidad and Tobago, Esperanza Road, Point Lisas, 540517, Trinidad and Tobago

Ragoobar, M., Alexander, D., & Bahaw, E. (2025). Optimization of a geothermal reservoir: A case study for Parryland Field. Journal of Smart Science and Technology, 5(2), 36-62.

ARTICLE INFO

Article history: Received 02 February 2025 Revised 14 April 2025 Accepted 02 June 2025 Published 30 September 2025

Kevwords: enhance geothermal system geothermal energy renewable energy carbon dioxide reduction economic analysis

10.24191/jsst.v5i2.110

ABSTRACT

The increasing global demand for energy and the pressing need for sustainable resource utilization have compelled societies to seek cleaner alternatives due to the rapid depletion of fossil fuels and environmental concerns. Despite having benefited substantially from its fossil fuel resources, the country of Trinidad and Tobago (TT) has fallen behind other Caribbean Nations in its transition to cleaner energy. Geothermal resources can be leveraged using existing infrastructure through the transformation of abandoned oil and gas wells into geothermal wells as an innovative, low cost means of advancing sustainable energy initiatives. This study focuses on optimising this transformation, using the abandoned Parryland Field in Southwestern TT as a case study. The initial geothermal reservoir model, constructed using the Computer Modelling Group (CMG) software, underwent key sensitivity analyses involving well spacing, injection rate, and the selection of working fluids. These analyses led to the development of an optimised model with the implementation of a retrofitted geothermal system, consisting of 3 injector wells and 3 producer wells which yielded 184.8 GWh of electricity over a 30-year period. In terms of the economic viability, the optimised configuration generated a positive Net Present Value (NPV) based on a deterministic cashflow model, which also predicted a favourable investment risk profile when subjected to Monte Carlo Simulations using the Crystal Ball software application by Oracle. Furthermore, harnessing the geothermal energy for power generation resulted in a reduction of 157.1 MMlbs of CO₂ emissions when compared with electricity produced using natural gas. This reduction is projected to occur over a 30-year period, facilitated by the utilization of 5.254 billion BTUs of enthalpy.

^{*} Corresponding author. E-mail address: melissaragoobar@yahoo.com https://doi.org/10.24191/jsst.v5i2.110



1 INTRODUCTION

Geothermal energy is not only sustainable but also renewable and clean, as it does not result in the emission of heat trapping greenhouse gases (GHGs)¹. The continuous heat generated within the Earth's crust, originating from the core, is harnessed to produce geothermal energy; a term derived from the Greek words geo (Earth) and therme (heat). As climate change occurs due to global warming, which was caused by the intensified accumulation of greenhouse gases (GHGs) in the atmosphere, there is a greater global impetus to switch to cleaner energy sources as nations are driven to explore alternatives to fossil fuel-based energy. This is done to fulfil increasing energy requirements whilst attempting to implement measures to mitigate greenhouse gas (GHG) emissions. This drive has spurred investigations into Enhanced Geothermal Systems (EGS) and the advancement of geothermal energy for electricity generation. Notably, EGS holds immense potential in contributing to long-term sustainable energy generation. However, for this potential to be fully achieved, the energy generated through EGS must remain economically viable.

Geothermal energy offers a continuous and dependable power source that remains unaffected by daily or seasonal variations, unlike other renewable options such as wind or solar energy. Its sustainability, flexibility, and reliability make it a valuable energy resource. Depending on the temperature of the extracted brine, geothermal energy can be effectively utilised for electricity generation, deep direct use, space heating and cooling, and various industrial applications². The majority of geothermal energy production and utilisation relies on naturally occurring high-temperature geothermal reservoirs. Such naturally occurring geothermal resources comprise three essential elements: a potent heat source often manifested in hot rock systems or magmatic intrusions; a fluid-filled reservoir intricately interconnected through subsurface conduits; and a permeability network to serve as a pivotal conduit for fluid flow³.

According to Schütz et al.⁴ notwithstanding the prevalence of high temperature reservoirs, there is significant untapped potential within lower temperature reservoirs, which are characterised by temperatures ranging from 100 °C to 200 °C (212 °F to 392 °F). These reservoirs which are often located at considerable depths, pose distinct technical challenges due to their insufficient natural permeability and fluid saturation. Consequently, innovative measures are imperative to unlock their full geothermal potential, which has significant implications for expanding the scope of geothermal energy production and as such they can be called manmade reservoirs (EGS)⁵.

The increasing demand for cleaner energy sources, driven by climate agreements and their associated targets, has prompted countries to explore various energy alternatives. The advancement of geothermal energy for electricity generation, particularly through EGS, is a promising option. According to the American Geoscience Institute, EGS has the potential to become a significant contributor to future energy sustainability⁶.

Although Trinidad and Tobago (TT) lacks conventional geothermal reservoirs like those in the neighbouring Lesser Antilles, the island possesses volcanoes and a significant number of abandoned oil and gas wells that can be adapted for geothermal energy production. Additionally, wellbore integrity must be intact, and production capacity must meet the necessary requirements for injection and production in an EGS as described by Mehmood et al.⁷. Forest Reserve contains hundreds of abandoned oil wells with shut-in temperatures ranging from approximately 100 °C to 115 °C (212 °F to 239 °F), that meet the necessary temperature gradient for EGS-applications.

According to Ritchie et al.⁸ climate change stands as one of the most significant global challenges facing humanity at present. As depicted in Fig. 1, a substantial and increasing volume of anthropogenic carbon dioxide (CO₂) and other greenhouse gases (GHGs) being emitted into the atmosphere by nations, which contributes to global warming and climate change.

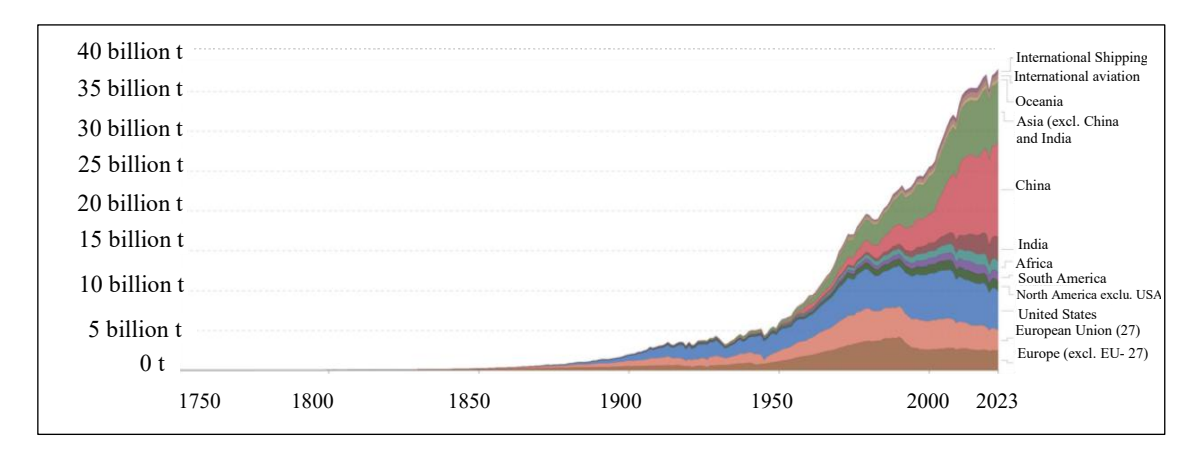


Fig. 1. Annual CO₂ emission from 1750 to 20238.

Fig. 2 illustrates the historical and projected trends in world energy consumption. With the expansion of the global population, the demand for energy increases in tandem with the prediction of a 28% rise between 2015 and 2040⁹. This shows that, over the forecast period, fossil fuels are still expected to provide the largest share of primary energy which, if left unaddressed, would lead to further increases in worldwide carbon dioxide emissions.

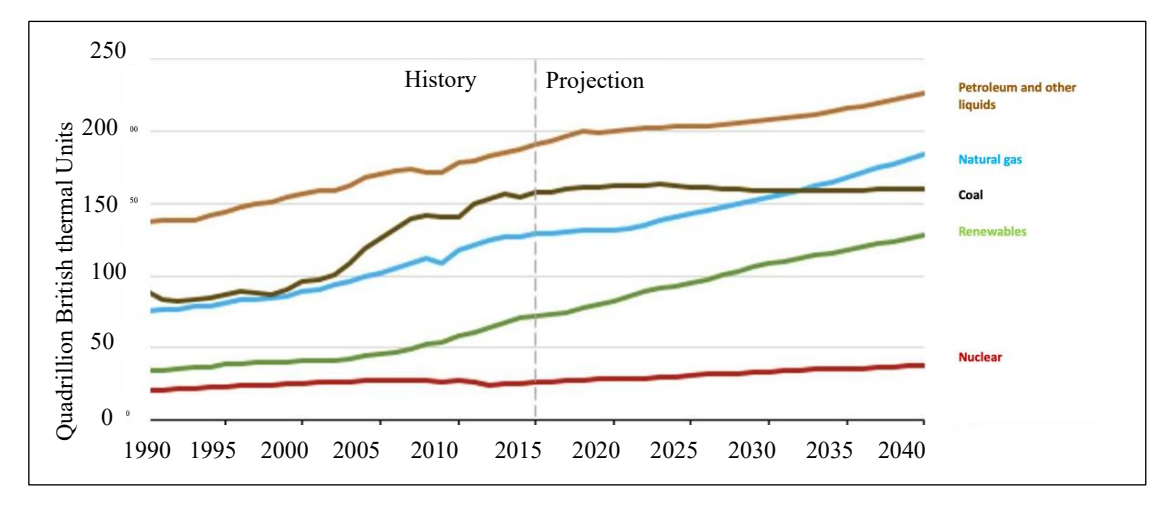


Fig. 2. World Energy Consumption by Energy Source 1990-20409.

TT, situated in the Caribbean, has reaped significant benefits from its fossil fuel reserves, where commercial production began in 1908 and currently remains ongoing. The oil and gas sector holds paramount importance, contributing to approximately 85% of total export earnings, 40% of government revenue, and over 35% of TT's gross domestic product (GDP)¹⁰. As illustrated in Fig. 3, back in 1992, the country's average daily oil production stood at 123,000 barrels whereas in 2022, it has dwindled to around 58,000 barrels per day, strongly highlighting the need for economic diversification away from hydrocarbons¹¹.

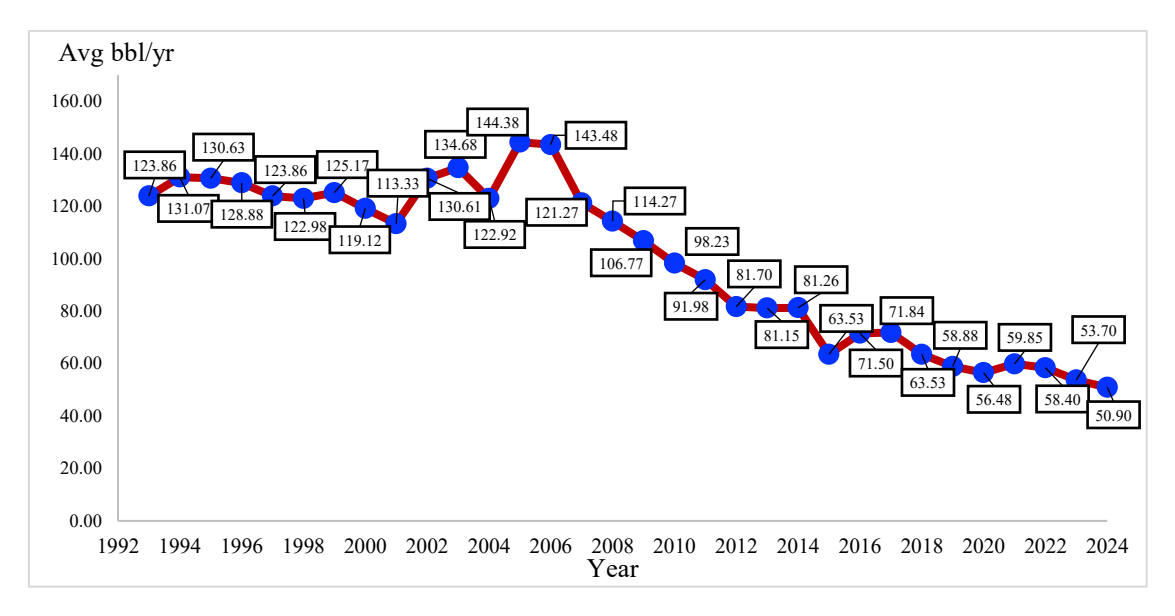


Fig. 3. Trinidad and Tobago's Crude Oil Production 1993 – 2024¹¹.

TT's significant carbon footprint and emissions reduction are now receiving a lot of attention and has been using oil and gas as its primary source of energy for more than 100 years ¹². According to Sun et al. ¹³ the global public is concerned about the energy crisis, global warming, and environmental pollution. Renewables are now widely accepted as mainstream energy sources all over the world. Crude oil, as the primary source of energy, will undoubtedly be heavily influenced by renewable energy sources in the future. According to the Paris agreement ¹⁴ it aims to make financial flows consistent with a low GHG emissions and climate-resilient pathway, as well as to increase countries' capacity to deal with the effects of climate change. TT have been classified as one of the highest greenhouse gas emitters per capita. Historically, the government of TT has been able to offer significantly discounted petroleum to its people. The eventual elimination of these subsidies necessitates diversifying the current energy mix and developing new energy sources¹⁵.

Geothermal energy has enormous potential, but its development and adoption have been comparatively gradual and limited to a small number of unique regions. Utilizing abandoned oil and gas wells is one possible answer to this issue. Since they are readily available, i.e., no drilling is necessary, and they typically have complete data logs throughout their production periods, abandoned oil/gas wells have a great potential to be converted into geothermal wells. This allows for complete well performance estimation, minimises risk, and yields a better cost estimation as described by Jello and Baser¹⁶. The expense of decommissioning an old oil well can be reduced or even eliminated with the conversion of an abandoned oil well into a geothermal well. The possibility of converting ageing, unprofitable oil and gas wells into geothermal wells grows as their number steadily rises over time as described in Tester et al. 17. As a result, the primary driver influencing the advancement of this technology is the reduction of drilling costs. Co-production or well conversion using exhausted and abandoned hydrocarbon wells for geothermal development is one possible remedy. An integrated hydrocarbon well system not only generates energy but also presents an opportunity to restore the wells, thereby reducing or eliminating any harmful environmental effects they may have caused as described by Jello and Baser¹⁶. A study conducted by Toth et al. ¹⁸ examined the potential of repurposing abandoned hydrocarbon wells in Hungary for hydrothermal or EGS applications. The study identified 168 wells, each approximately 1,000 meters deep, with bottom-hole temperatures ranging from 40 °C to 69 °C (104 °F to 156.2 °F). These wells extended into sedimentary formations and were located in areas with moderate to high terrestrial heat flow. Based on these conditions,

the study concluded that the wells were well-suited for low-temperature direct-use applications such as district heating, greenhouse cultivation, and aquaculture.

Geothermal energy can produce, store, and generate electricity continuously. Geothermal power plants can run at full capacity day and night since the energy source is constant. Compared to less than 30% for wind power and less than 15% for solar Photovoltaics (solar PV), the average global geothermal capacity utilisation rate in 2023 was over 75%. Furthermore, the flexibility of geothermal power plants' operations helps stabilise electrical grids by guaranteeing that demand can always be satisfied and facilitating the incorporation of variable renewables like wind and solar PV¹⁹.

The fact that replacement wells are frequently required to compensate for declining productivity at existing wells is a crucial factor for geothermal power facilities²⁰. Fluid must be injected back into subterranean reservoirs quicker than it is being used up in order to ensure the sustainability of geothermal energy. This implies that, to remain sustainable, geothermal energy must be managed efficiently²¹. According to Kurnia et al.²², prior to well conversion, trustworthy screening and preprocessing are recommended. For example, wells should have a permeable reservoir, a reasonable geothermal gradient, a sufficient depth, and a consistent temperature output throughout the project's duration.

Hydrocarbon wells are typically dispersed across remote locations with minimal access to infrastructure including roads and basic services. This creates an extra hurdle for repurposing efforts, as ensuring the presence of readily available operating staff and technicians becomes more challenging. According to Maurel et al.²³, a number of operational concerns must be taken into account while repurposing a well for geothermal energy recovery. To name a few, a hydrocarbon well's design could not be suitable for geothermal uses, resulting in technological challenges that would render the conversion unfeasible. Additionally, a number of criteria should be evaluated to guarantee the endurance of exploitation, including the well's casing and cement integrity, wellbore aging, and sealing the borehole from nearby formations and aquifers. Evaluating older wells may pose challenges. Additionally, there is an operational risk related to incorrectly identifying the geological profile. Numerous uncertainties in geothermal projects stem from an inadequate evaluation of the potential maximum flow rate, the temperature of the fluid, and the heat capacity of the formations. A drawback to retrofitting an abandoned oil field in this way, would be that it prevents the implementation of EOR—with possible future improvements in technology to extract the remaining oil in place, which therefore makes such reserves stranded.

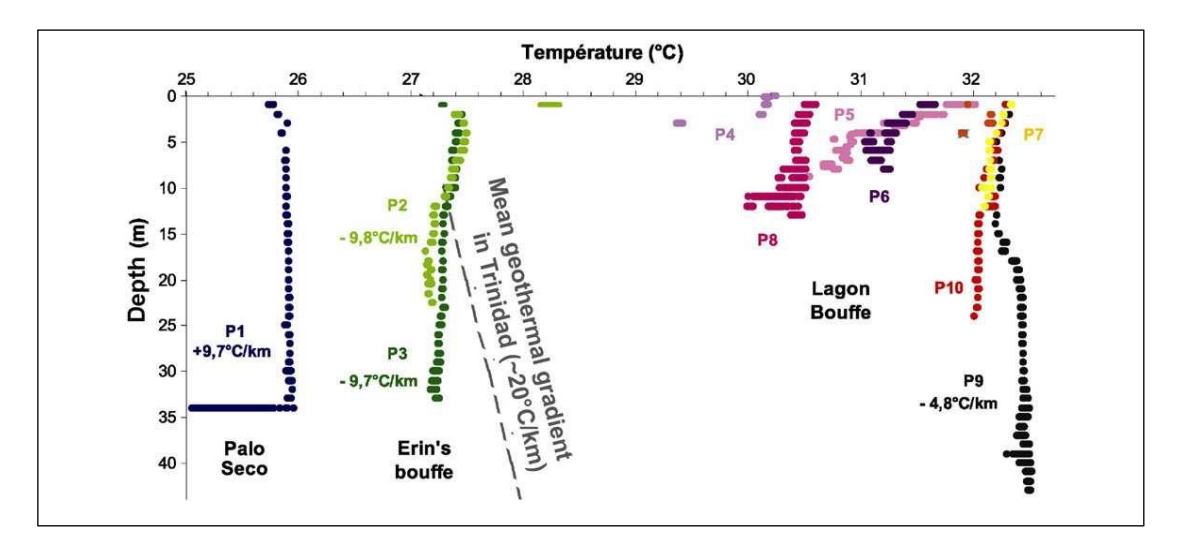


Fig. 4. Temperature Profiles Recorded in Conduits of Several Mud Volcanoes in Trinidad²⁴.

The support for this country's thermal potential is evident from mud volcanoes in its Southern region and diverse geothermal gradients. According to Deville and Guerlais²⁴, the identification of geothermal hotspots exhibiting temperature gradients of 89.6 °F km⁻¹ (32 °C km⁻¹), surpassing the typical geothermal gradient for TT ranging from 68 °F km⁻¹ (20 °C km⁻¹) to 73.4 °F km⁻¹ (23 °C km⁻¹), presents promising indications for harnessing geothermal energy as shown in Fig. 4.

The comparatively negligible carbon emissions from geothermal energy, combined with its high-capacity factors (above 90%), make it an attractive source of energy. This enables the plants to operate continuously, making them better producers of a more predictable and stable supply of baseload electricity and heat than other renewable sources such as solar and wind. Exploiting geothermal energy in the Caribbean can be crucial to achieving goals for energy security, economic growth, and climate change mitigation. This resource can be used to produce electricity and other direct uses by utilizing the thermal energy that has been trapped within the rocks, as described by Dickson and Fanelli²⁵.

2 METHODOLOGY

Data for input values was gathered through secondary sources from past studies on the Parryland field as well as other studies based on locations near the Parrylands area in Southwestern Trinidad which serve as analogs. Fig. 5 presents a flow chart outlining the steps of the methodology. The initial step involved acquiring the geological description of the reservoir area by analysing well log data from the field, which included information such as the structure map, permeability, and porosity. This data was then utilised to construct the reservoir simulation model. Natural fracture modelling was employed to create the non-single porosity, homogeneous model, as described by Bell-Eversley et al.²⁶. In the third step, mathematical modelling was conducted based on the methodology of Patihk et al. ²⁷. Several well configurations and patterns, including five-spot and staggered line drive arrangements, were simulated using CMG software. The potential of utilizing CO₂ as a geothermal working fluid was also investigated by altering the fluid properties within the software to reflect the characteristics of CO₂.

The optimal model was then identified after completing all sensitivity analyses. This model was then used to calculate CO_2 emissions based on standard emission factors for natural gas and geothermal power plants, as outlined by Bloomfield and Moore²⁸. The total emissions were determined by multiplying the total energy production in kilowatt-hour (kWh) by the emission factors, enabling the calculation of CO_2 reduction potential.

In the final step, an economic analysis was conducted following the method described by Bell-Eversley et al.²⁶. Capital expenditures (CAPEX) and operational expenditures (OPEX) were calculated, and revenue was estimated using the electricity rate charged by the Trinidad and Tobago Electricity Commission (TTEC) to residential users. These values were used to calculate the net present value (NPV) and internal rate of return (IRR) to assess the project's economic feasibility. A minimum acceptable rate of return (MARR) of 10% was set as the criteria for feasibility.

This study explores the feasibility of utilizing geothermal energy in Trinidad and Tobago by developing a hypothetical model based on real-world data from reservoirs in the Parrylands Area. This investigation examines key factors influencing energy production, including optimal spacing between injector and producer wells, injection rates, and the selection of working fluids. It also assesses the potential reduction in CO₂ emissions when geothermal energy is used as an alternative to fossil fuels. The research aims to evaluate both the technical and economic viability of geothermal energy deployment in TT while highlighting its environmental benefits. Additionally, this study proposes the use of wells from an abandoned oil field to implement a geothermal energy system, thereby reducing capital expenditure by eliminating the need for new drilling. These cost saving initiatives can contribute to a lower cost per kilowatt-hour (kWh) of clean, renewable electricity.

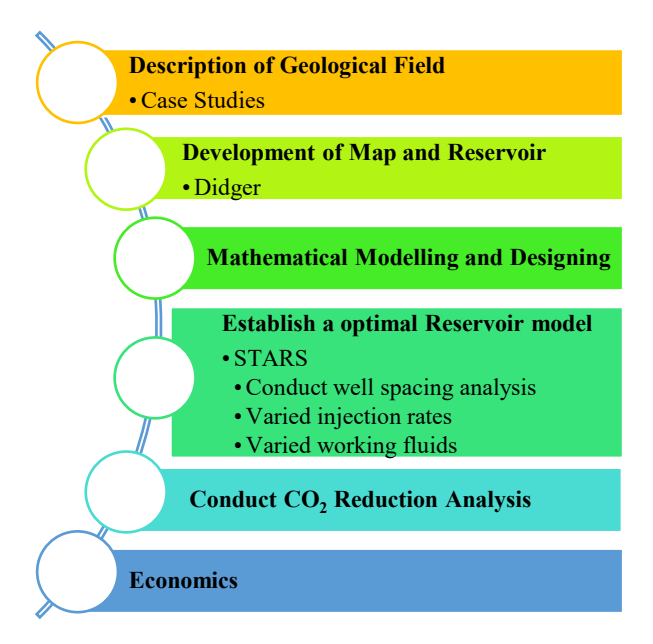


Fig. 5. Flow Chart showing Methodology of the study.

2.1 Field description

This field, which was previously the site of steam flooding projects, is located north of the Los Bajos fault system, along the northern side of the east-west trending Point Fortin anticline. The area currently contains hundreds of abandoned wells, as shown in Fig. 6²⁹. There are several key characteristics of the field which have influenced the development of the geothermal models. The reservoir is made up of Cruse 'E' Sands, the Late Miocene to Early Pliocene-aged. Cruse Formation consists of sandstones, claystones, and silt stones originating from basin floor and slope fan deposits. It is important to note that this specific field underwent steam flooding during its hydrocarbon production phase.

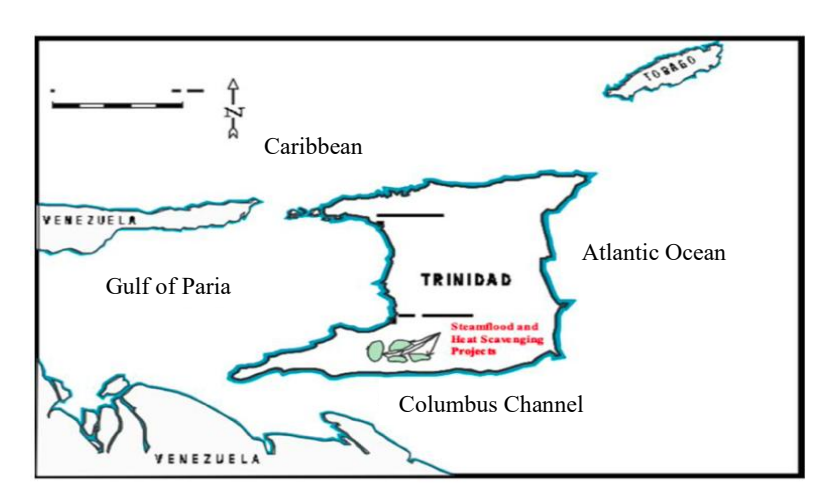


Fig. 6. Steam flooding in Parrylands Area²⁹.

The Upper Cruse, characterised by dark grey, non-calcareous shale, contains irregular nodules of hard grey clay-stone³⁰. According to Ramlal²⁹, the Lower Cruse is dominated by gypsiferous clays that

range in colour from grey to black, weathering from brownish-yellow to red. These clays intermingle with silty clays, silts, and sandstone layers, progressively coarsening into the thick sandstone units of the Upper Cruse.

The Cruse sands are overlained by the Lower Forest clay shale layer. These sand blocks comprise complexes of distributary channels and mouth bars, oriented from North-East to South-West orientation and deposited within a lower deltaic plain. Notably, in Fig. 7, well log data was collected from the field indicates distinct shale units separating these reservoirs, alongside evident sand growth, particularly in units B and C. The well type log displays seven separate layers made up of interbedded shale and sand, which help in the creation of the reservoir model in CMG.

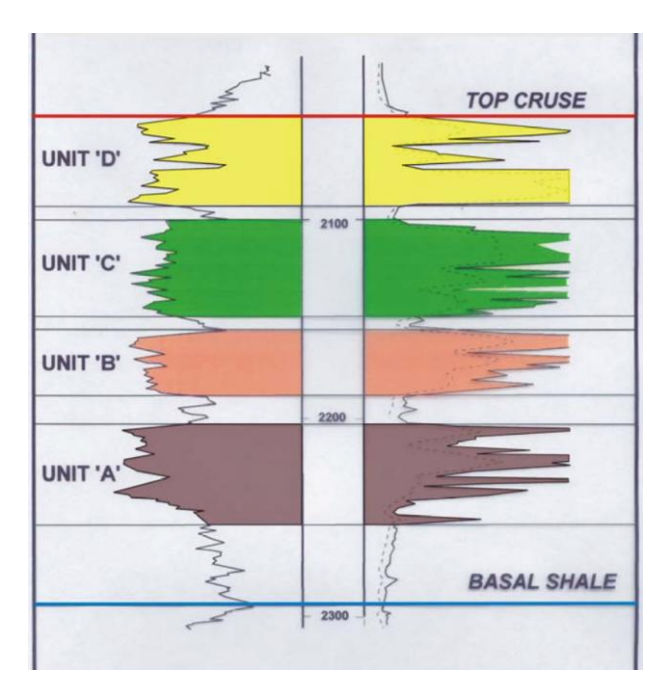


Fig. 7. Well Log Data obtained in Cruse Sands²⁹.

2.2 Map and reservoir development

The generation of both the structural map and geothermal reservoir models was created and digitized through the utilization of Didger and CMG software. In the process of reservoir development, the structural map and contours of the net oil sand isopach maps, sourced from a previous study conducted by Ramlal²⁹ on the Parrylands Area was digitised. This approach enhances the accuracy of assessing the reservoir's volumetric attributes. The acquired data facilitated the measurement of sand and shale unit thicknesses, which are subsequently incorporated into the CMG modelling program. Table 1 shows the parameters specific to the Parrylands Area²⁹.

Table 1. Parameters used in geothermal model²⁹

Parameter	Value
Depth to top of sand	2050 ft
Permeability	265 mD
Porosity	31%
Sand Thickness	75 ft

2.3 Mathematical modelling

To investigate thermal recovery mechanisms, a three-dimensional numerical geothermal model was utilised, incorporating the premise of local thermal non-equilibrium. The adapted geothermal system will employ energy equations to compute the present-field temperature of the fluid within the fractured rock matrix. Subsequently, the heat transfer process between the actual rock and fluid during heat retrieval will be depicted through the representation of the temperature field as outline by Patihk et al.²⁷.

2.4 Mass conservation

According to Liang et al.³⁰, and Zhu et al.³¹, the fluid flow through a material with variable porosity is depicted by the mass balance equation, which is set by Equation 1.

$$S\frac{\partial p}{\partial t} + \nabla \cdot u = -\frac{\partial e}{\partial t} + Q \tag{1}$$

where S, P and t stand for constrained specific storage of the media, pressure, and time, respectively; e stands for volumetric strain; and Q stands for the source-sink of the outflow process. As long as the water flow rate, u, abides by fluid flow's Darcy's Law, the following Equation 2 can be said:

$$u = -\frac{k}{\mu} \left(\Delta p + \rho_f g \, \nabla z \right) \tag{2}$$

where permeability of the saturated porous medium is denoted by k, dynamic viscosity and fluid density are denoted by μ and ρ_f respectively, gravitational acceleration is denoted by g, and the course of gravity is denoted by the unit vector z.

Using Equations 3 and 4, the mass balance equation for fractures is computed as outline by Liang et al.³⁰, and Zhang et al.³²

$$d_f S_f \frac{\partial p}{\partial f} + \nabla t. u_f = -\partial_f \frac{\partial ef}{\partial t} Qf \tag{3}$$

$$u_f = -d_f \frac{\kappa_f}{\mu} \left(\nabla_t \rho + \rho_f g \nabla_t z \right) \tag{4}$$

where S_f , Kf, d_f and ef refers to the specific storage, permeability, thickness and the volumetric strain of fractures respectively; ∇_t refers to the gradient operator; and Qf refers to the fluid flow in the fractures as in Equation 5. The fracture surfaces is represented by m.

$$Qf = -\frac{\kappa_f}{\mu} \frac{\partial_p}{\partial_m} \tag{5}$$

2.5 Rock mass temperature field

According to Zhang et al.³² the lower porosity will result in a low water velocity in the rock matrix, it is expected that the water temperature will be equal to the rock temperature.

$$C_s \rho_s \frac{\partial T_s}{\partial t} = \lambda_s \nabla^2 T_s + W \tag{6}$$

where ρ_s denotes the density of the rock; λ_s denotes the rock matrix thermal conductivity; C_s is the rock heat capacity and "W" denotes the heat exchange that occurs in the reservoir; a negative sign denotes heat that has been drawn from the rock, and a positive sign denotes heat that has been drawn into the fluid. https://doi.org/10.24191/jsst.v5i2.110

2.6 Water temperature field

$$d_f \rho_f C_f \frac{\partial T_f}{\partial t} + d_f \rho_f C_f u_f \nabla_f T_f = d_f \nabla_f (\lambda_f \nabla_f T_f) + W_f$$
(7)

In Equation 7, ρ_f , C_f and λ_f represents the density, heat capacity, and thermal conductivity of water; u_f and T_f signifies the water flow's velocity and the water's temperature inside the cracks; W_f stands for the heat that the water from the matrix block on the fractured surface has been able to capture as outlined by Zhang et al.³².

It is assumed that water obeys Newton's rule of heat transfer during the heat exchange between it and the rock matrix and fractures. Equation 8 describes the heat transport from the rock to the fracture fluid (water per unit area) as outlined by Xu et al³³.

$$W = h\left(T_s - T_f\right) \tag{8}$$

At the fracture surface, the temperatures of the water and the rock are identical when the convection efficiency h is high enough.

2.7 Fluid properties under high temperature and pressure

According to Xu et al.³³, the fluid density ρ^f (water density), which may be characterised as a function of temperature and pressure becomes variable and meets the following conditions in the deep geothermal reservoirs when temperature and pressure are high enough as shown in Equation 9.

$$\frac{1}{\rho_f} = 3.3086 - 0.899017 (4015.15 - T)^{0.147166} - 0.39 (658.15 - T)^{-1.6} (p - 225.6) + \delta$$
 (9)

where δ denotes the function of water temperature T and pressure p; δ typically remains below 6% of $\frac{1}{\rho_f}$ which then influences the dynamic viscosity $\mu = v\rho_f$, where v denotes the kinematic viscosity of water.

Initial and boundary conditions

The heat output of the modified geothermal system was simulated in accordance with the initial and boundary conditions. The investigation spanned a 30-year timeframe, employing time steps of one month. The injection well pressure was held constant at 1,300 psi, while the bottomhole pressure was sustained at 1,000 psi, ensuring continuous water circulation within the intended reservoir. The Heat Flux (Qs) remained consistent, with the surface temperature of the injection well set at 68 °F (20 °C).

Adopted parameters that are utilized in the computations

Although Trinidad and Tobago have not yet discovered any geothermal reservoirs within its territory, this research can be applied to understand and predict the behaviour of geothermal systems with similar geological and reservoir characteristics, once such resources are identified. The reservoir temperature was estimated based on the assumption that a hypothetical geothermal reservoir exists near a known geothermal hotspot in Trinidad, where geothermal gradients have been reported to reach up to 32 °C km⁻¹ as described by Deville and Guerlais²⁴. A study conducted by Fofinha³⁴ states that binary power plants can operate using lower-temperature geothermal fluids within the range of 100 °C to 170 °C (212 °F to 338 °F). However, when fluid temperatures fall below 100°C (212°F), the efficiency of electrical energy generation significantly declines. As such, a base case reservoir temperature of 100 °C (212 °F) was

selected, as temperatures below this threshold are generally considered non-viable or inefficient for power production.

The information displayed in Tables 2, 3, and 4 demonstrates the adopted parameters that were utilised in the computations.

Table 2. Adopted parameters

	Parameter	Values	Unit
	D 4 6	2050	ft
	Depth of reservoir	0.465	psi/ft
	Pressure gradient	31	%
Reservoir	Matrix porosity	265	mD
	Permeability in I direction	265	mD
	Permeability in J direction	0.1	
	Kv/Kh		
	Fracture porosity	0.0062	
	Permeability in I direction	2560	mD
.	Permeability in J direction	2650	mD
Fracture	Kv/Kh	2	
	Fracture Spacing, I	32.8084	ft
	Fracture Spacing J	32.8084	ft
	Fracture Spacing K	0	ft
	Rock Compressibility	3.173×10^{-6}	1/psi
	Porosity Reference Pressure	635.5	psi
- I	Thermal Conductivity reservoir rock	49.6	Btu/(ft*day*°F)
Thermal	Thermal Conductivity Water	8.330	Btu/(ft*day*°F)
	Volumetric heat capacity	37.2767	$Btu/(ft^3*^oF)$
	Critical Temperature	705.038	°F
	Molecular Weight	18.02	lbmole/lbmole
Reservoir Fluids	Molar density	3.4637	lbmole/ft ³
	Liquid Compressibility	5.06×10^{-6}	1/psi
	1st thermal expansion	0.000488889	1/F

Table 3. Adopted saturation input parameters

	Sw	krw	krow
1	0.01	0	1
2	0.99	1	0

-	SI	krg	krog
1	0.01	1	0
2	0.99	0	1

Table 4. Adopted relative permeability parameters for fracture

Geological Properties	Values	Unit
OWC	2250	ft
Reservoir Temperature	212	°F
Fractured Temperature	212	°F
Reference pressure	635.5	psi
Reference Depth	2050	ft

Carbon dioxide equation

There were two fundamental methods for assessing CO_2 emissions from stationary sources: direct measurement and fuel input analysis (U.S Environmental Protection Agency 2008)³⁵. For the purposes of this study, the Fuel Input Analysis approach was chosen, following the methodology outlined by Boodlal et al.³⁶, Equation 10 illustrates the general formula equation for the calculation, outlining the individual components of the equation.

Emissions =
$$\varepsilon_{i=1}^n = Fuel_i \times HC_i \times C_1 \times FO_i \times \frac{cO_2}{C_{(m,w)}}$$
 (10)

where $Fuel_i$ = mass of volume of fuel Type i combusted, HC_i = heat content of fuel type i, (energy per mass or volume of fuel), C_1 = carbon content coefficient of fuel type i (Mass C / Energy), FO_i = fraction of oxidized fuel type i, CO_2 (m.w.) = molecular weight of CO_2 , C (m.w.) = molecular weight of carbon.

This study is limited by the simplifying assumption that the reservoir temperature is 212 °F as well as the structural integrity of the aged wells are suitable for accommodating the installation of geothermal energy infrastructure. As such, a real-world application of this concept requires a thorough assessment of the wells and reservoir. In addition, there are limitations due to the exclusion of consideration to both water supply and cost of substation connectivity.

3 MODEL SIMULATION

The reservoir model was created using the data from Tables 1, 2, 3 and 4 in CMG STARS (2022). Two different EGS set-ups were numerically simulated for this analysis a staggered line drive, and an inverted five-spot. At 68 °F (20 °C room temperature) the porosity and permeability values were 31% and 265 millidarcies. The investigation involved examining different injection rates, well patterns and working fluids.

The reservoir model was established using a sandstone layer with a depth of 2,050 feet with the numerical 3D model dimension of 69 ft \times 51 ft \times 7 ft with a thickness of 100 ft. The reservoir has been fully perforated, spanning from the uppermost to the lowermost layers. To optimise the utilisation of the formation's energy, the producer well was operated with a minimum bottom-hole pressure of 1,000 psi. A consistent water injection process was initiated and maintained for a duration of 30 years.

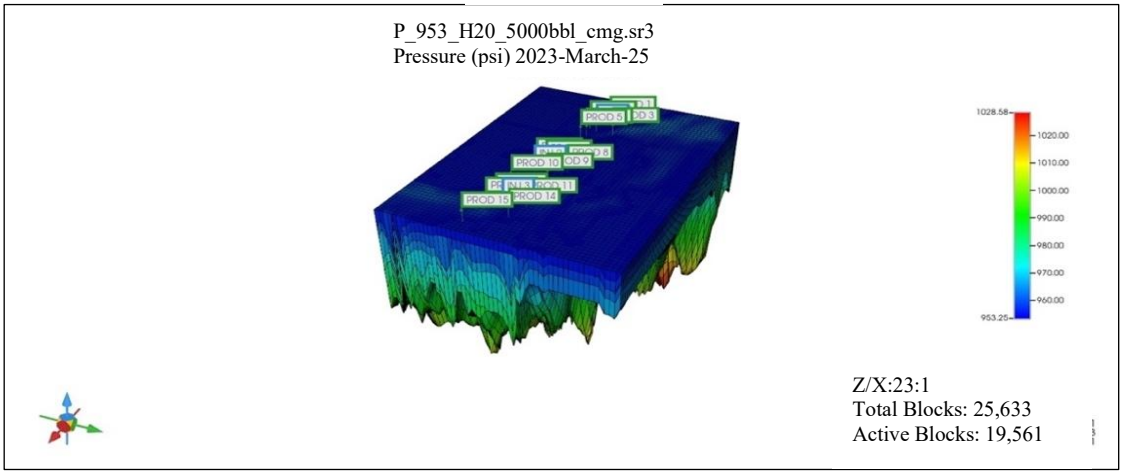


Fig. 8. Inverted 5 spot well.

Initially, the base model was modified and consisted of four (4) injectors and four (4) producers. There is one (1) vertical injector and four (4) vertical fractured producers for the inverted 5-spot well layout as shown in Fig. 8. The well pattern was then adjusted to a staggered line drive depicted in Fig. 9, with three (3) producers and three (3) injectors with all the data values remaining constant. The cumulative enthalpy for 30 years was 5.10727×10^{12} BTU showed that this change in the well pattern resulted in an increase in thermal recovery and the well spacing was then varied based on the staggered line drive. According to the findings, the injection flow rate, well spacing and working fluids have the biggest impacts on the total heat extraction.

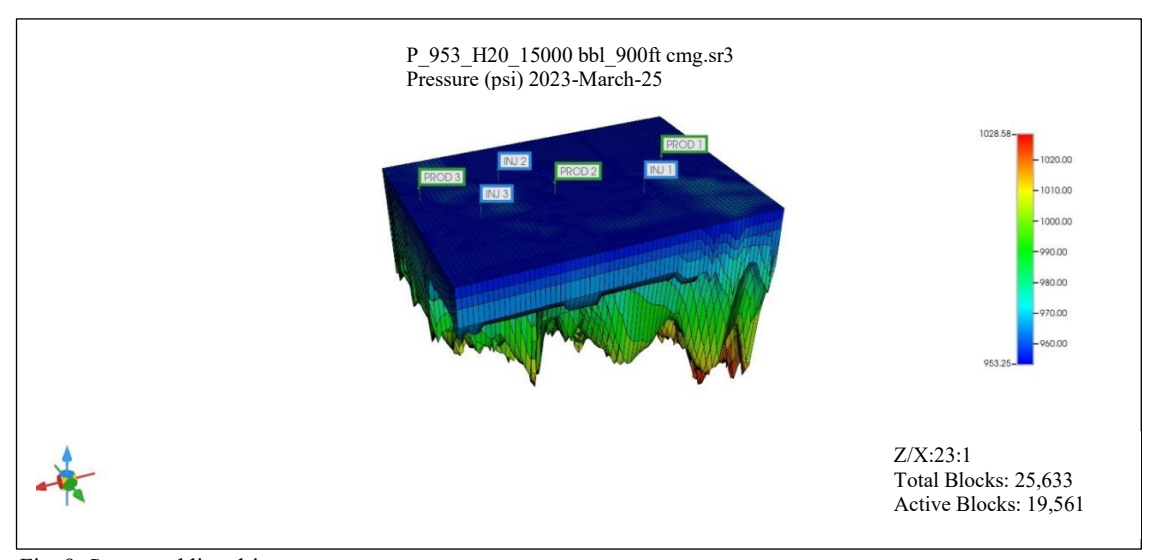


Fig. 9. Staggered line drive.

4 ECONOMIC MODEL

Using the result of the simulations from CMG which provided a forecast of the recoverable heat from the reservoir over the 30-year duration, the amount of electricity which could be generated from the geothermal system was calculated and placed into a deterministic economic model, which incorporated the selling price of electricity together with the associated Capital Expenditure (CAPEX), Operating Expenditure (OPEX) and Taxes to determine the net cashflows of the investment. The Net Present Value (NPV) was then calculated using a minimum acceptable rate of return of 10% and Monte Carlo Simulations were then applied to the deterministic model to assess the impact of varying the price of electricity, CAPEX and OPEX as well as energy conversion efficiency on the feasibility of the investment.

5 RESULTS AND DISCUSSION

A mathematical model for a geothermal reservoir was constructed, utilizing geological data obtained from a reservoir in the Parryland field with a depth of 2,050 feet uppermost sand layer. The assigned injection pressure was set below the fracture threshold of 1,435 psi which was determined by multiplying the fracture pressure gradient of 0.7 psi per ft by the depth.

5.1 Well spacing analysis

Various well spacings from 500 ft with a well spacing of 200 ft interval were experimented while retaining a consistent injection pressure of 1,300 psi and a constant injection rate of 10,000 barrels per day. These fluctuations attributed to the interaction between injected water and the formation. As well spacing expands, this direct connection between well spacing and cumulative enthalpy slowly decreased. As water

travels towards the producer under consistent pressure, it gains more time to exchange heat with the formation, thus absorbing energy.

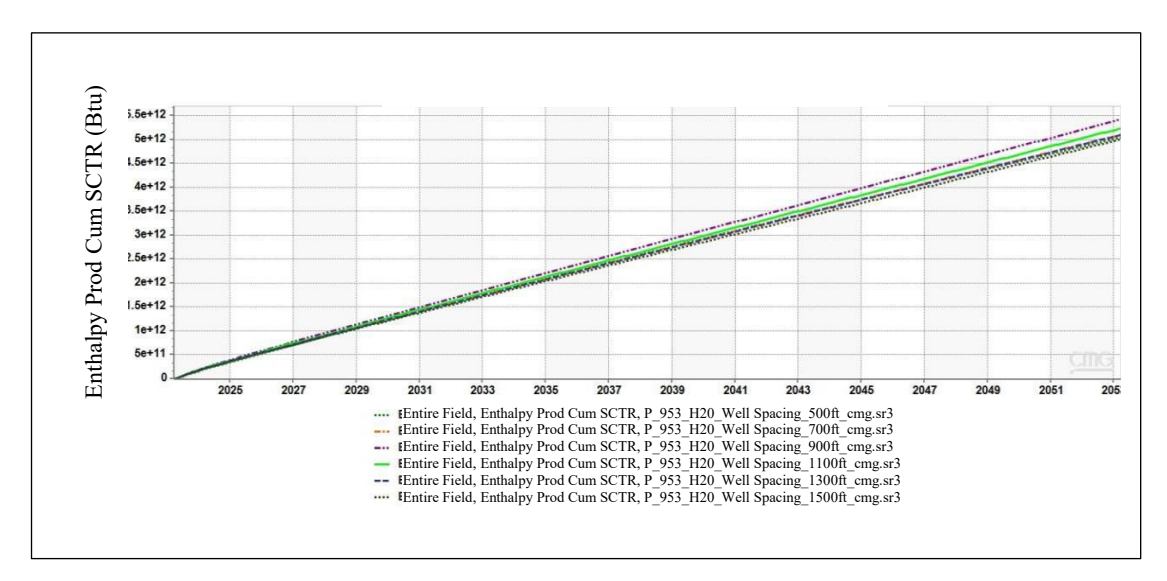


Fig. 10. Well spacing enthalpy prod cum for a period of 30 years (unit Btu).

As depicted in Fig. 10, the efficiency of geothermal energy production in this model is largely influenced by three key factors: the spacing between injector and producer wells, the injection rate, and the type of working fluid selected. At an injection rate of 10,000 bbl per day, the simulation showed that a well spacing of 500 ft produced a cumulative thermal output of 5.04577×10^{12} Btu. This increased to 5.10413×10^{12} Btu at 700 ft, peaking at 900 ft with 5.42665×10^{12} Btu. Beyond this distance, thermal output began to decline—yielding 5.22440×10^{12} Btu at 1,100 ft, 5.09967×10^{12} Btu at 1,300 ft, and dropping further to 4.99409×10^{12} Btu at 1,500 ft.

This behaviour suggests that wider well spacing gives injected water more time to interact with the reservoir rock, enhancing heat transfer under continuous pressure. However, as water approaches the production well, it travels faster, reducing the window for effective thermal exchange and energy absorption, which in turn leads to decreased enthalpy. Although a general trend can be observed, the relationship between well spacing and heat recovery is subjected to operational limitations and subsurface variability.

Specifically, for well spacings beyond 900 ft, the cumulative enthalpy output began to decline, likely due to the reduced ability of the injected water to sufficiently influence the production wells and sustain reservoir pressure. Fluid losses become more pronounced at greater distances between wells, whereas they are less significant when wells are positioned closer together. Therefore, to maximize reservoir performance and energy yield, careful consideration must be given to optimising both the output flow rate and the well spacing. Based on the model, the ideal configuration for a staggered line drive setup is a well spacing of 900 ft, with an injection pressure of 1,300 psi and an injection rate of 10,000 bbl per day.

5.2 Injection rate- staggered line drive

The well configuration in this scenario mirrors a straight-line setup, with the exception that the injectors are laterally displaced by a distance of a/2, as outlined by Doghaish³⁷. To maintain consistent reservoir pressure in the staggered line drive arrangement, a layout consisting of three injectors and three producers was utilized. This setup allowed for the examination of four different injection scenarios by varying the injection rates: 5,000 bbl per day, 10,000 bbl per day, 15,000 bbl per day, and 20,000 bbl per day, while keeping the well spacing fixed at 900 feet.

At 5,000 bbl per day, the average reservoir pressure was recorded at 1131.35 psi, while at 10,000 bbl per day, it was slightly lower at 1126.30 psi. Increasing the injection rate to 15.000 and 20.000 bbl per day resulted in minimal changes in pressure, as illustrated in Fig. 11. These results suggest that injection rate had a relatively minor influence on reservoir pressure behaviour, likely due to the dominant effect of the reservoir's baseline injection pressure.

Among the rates tested, 15,000 bbl per day emerged as the most efficient. As shown in Fig. 12, over a 30-year period, the peak cumulative heat output reached 5.42784×10^{12} Btu at this rate. In comparison, the heat outputs at 5,000, 10,000, and 20,000 bbl per day were 5.10727×10^{12} Btu, 5.42665×10^{12} Btu, and 5.41470×10^{12} Btu, respectively. This indicates that 15,000 bbl per day provided the best performance in terms of thermal energy recovery under the given reservoir conditions.

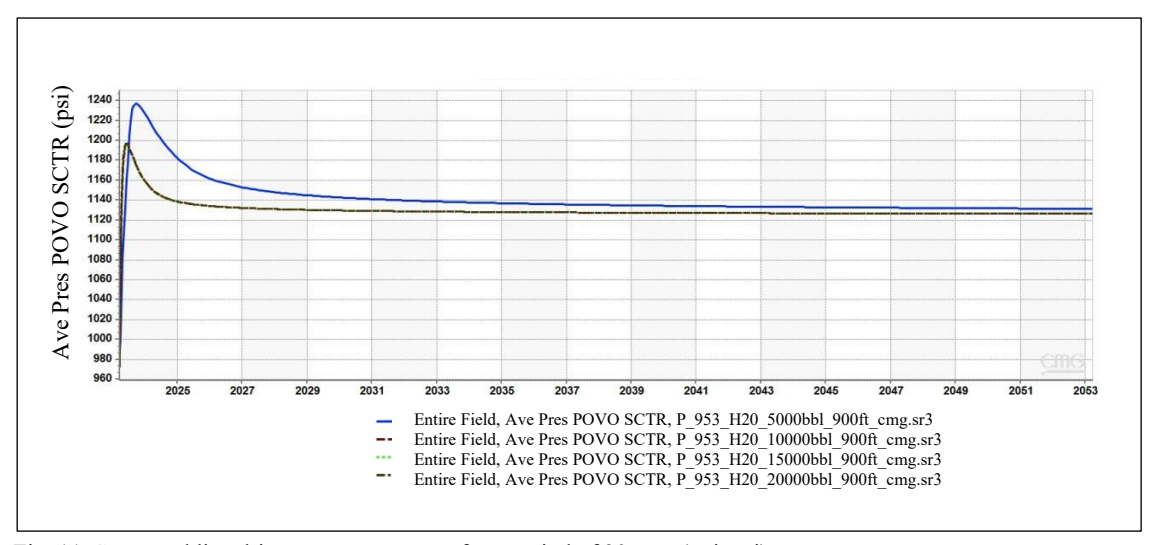


Fig. 11. Staggered line drive average pressure for a period of 30 year (unit psi).

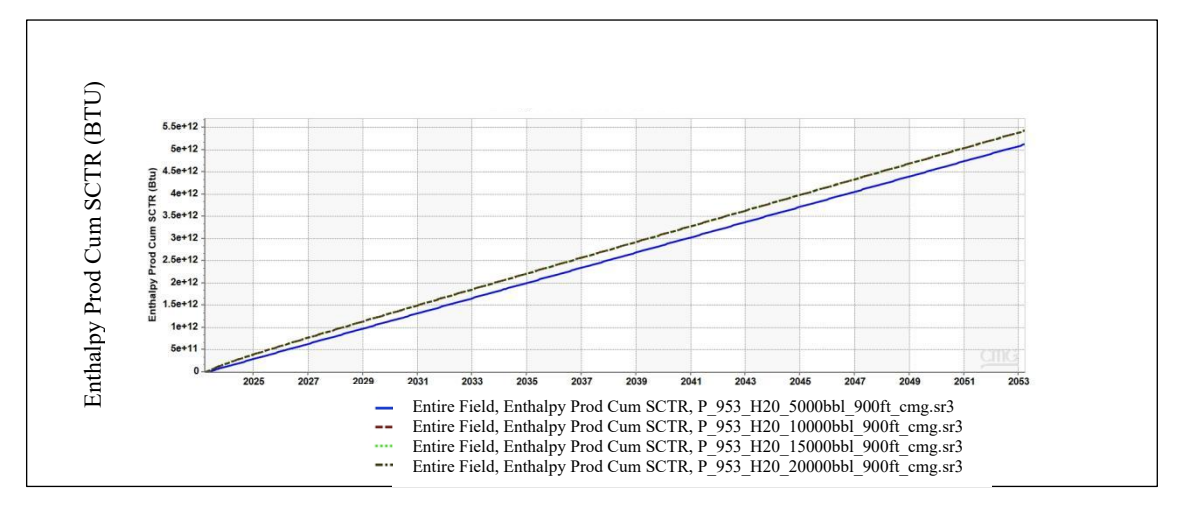


Fig. 12. Staggered line drive enthalpy prod cum for a period of 30 years (unit btu).

5.3 Applicable power generation capacity

The power generation capacity is determined using the optimal heat model, which assumes the injection of 15,000 barrels per day at 1,300 psi, utilizing 3 injection wells and 3 producer wells, with a well

©Authors, 2025

spacing of 900 ft. The simulated annual heat from this model over the 30-year period, from 2023 to 2052, is illustrated in Fig. 13. It is assumed that all infrastructure work will be completed by 2025, allowing for geothermal energy capture starting in 2026.

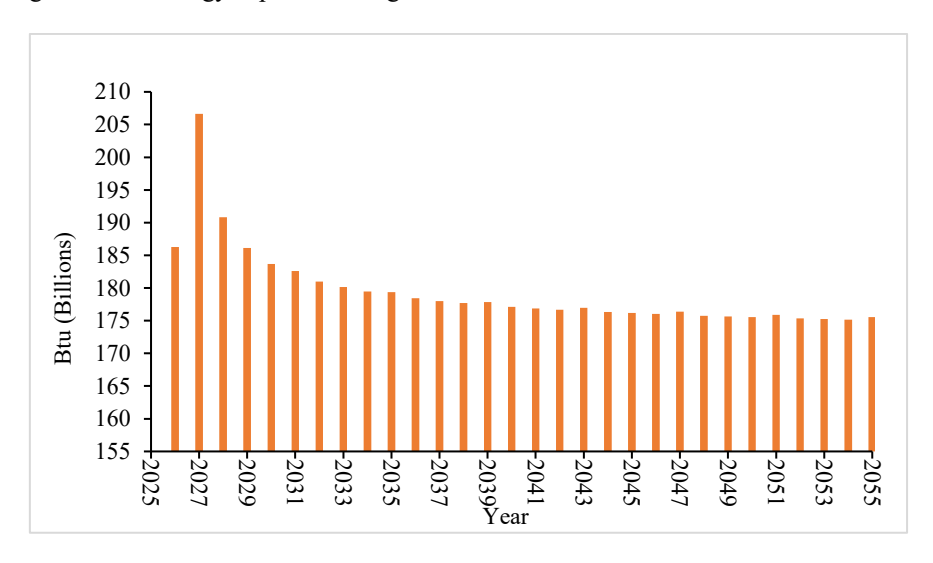


Fig. 13. Annual heat from best model (Unit Btu).

This shows that a rapid buildup is experience which soon peaks in 2027 followed by a rapid decline at first which subsequently slows considerably with an almost constant annual heat being generated in the later years up to 2052. The cumulative heat from this simulation over the period amount to 5.385 trillion Btu. Using a binary open loop cycle geothermal power plant this annual heat would be used to generate steam to drive a turbine which in turn would power an electricity generator in combination with other needed infrastructure such as a cooling tower and a separation tank. Typically, independent power producers sell electricity to the power distributor under a power purchase agreement with a fixed annual energy supply quota. In this paper it is therefore assumed that this quota would be based on the minimum heat in a given year over the forecast period which corresponds to 175.1 billion Btu in 2051. Overall, the heat utilized for electricity generation over the 30-period would amount to 5.254 trillion Btu or 97.6% of the total heat generated. This amount of energy would be capable of providing consistent electricity to approximately 5,254 homes.

According to Zarrouka and Moon³⁸ the average efficiency in electricity generation from geothermal energy is 12%. Based on this, the annual 175.1 Billion Btu of geothermal energy would generate 6.2 GWh of electricity each year over the period 2023 to 2052 using the conversion factor of 1 Btu is roughly equivalent to 0.000293071 kWh³⁹. This totals up to 184.8 GWh over the 30-year period which represents an electricity power capacity 0.7MW. Geothermal projects are classified as compact, with a land requirement ranging from 1 to 8 acres per MW⁴⁰. In the most expansive scenario, where eight acres are allocated per MW, the total land area would be approximately 5.6 acres.

5.4 Effect of working fluid

Water is typically used as the primary working fluid in conventional EGS due to its abundance and high heat capacity. However, a significant challenge with using water in EGS is the issue of water loss. Recent research by Liu et al.⁴¹ has explored the injection of CO₂ as an alternative in both water-based and CO₂-based methods, alongside the reinjection of pure water to maintain reservoir pressure stability.

Injecting CO₂ into a geothermal reservoir serves several functions, such as sustaining pressure, generating an artesian flow of brine, and increasing CO₂ storage capacity by creating additional space through the extraction of hot water. This approach can also improve porosity and permeability by enhancing

water-rock interactions, potentially increasing the geothermal reinjection efficiency of cooled return water in sandstone reservoirs.

The analysis of CO₂ as a geothermal working fluid, replacing traditional water, presents several compelling advantages that enhance geothermal energy extraction. The study's findings indicate that CO₂ not only increases cumulative enthalpy over the project duration but also demonstrates a superior thermal extraction rate compared to water when operating under identical well pressures. This aligns with previous research by Pruess⁴² and Liu et al.⁴³, reinforcing the potential of CO₂ in geothermal applications.

From a chemical standpoint, CO₂'s weaker solvent properties, in comparison to water, result in a lower tendency for mineral dissolution within the geothermal reservoir. This is advantageous as it reduces the risk of altering the reservoir's mineral composition, promoting long-term stability and sustainability of the geothermal system. The physical properties of CO₂ also contribute to its effectiveness as a geothermal fluid. Its higher compressibility and expansivity mean that less energy is needed for circulation, potentially reducing operational costs. Furthermore, CO₂'s lower viscosity allows for smoother flow through the reservoir and fractured formations, enhancing the efficiency of heat extraction⁴².

Another key benefit of using CO₂ is its potential for carbon sequestration. Any CO₂ losses during the geothermal process can help reduce greenhouse gas emissions, aligning geothermal energy production with climate change mitigation goals. This dual advantage of energy extraction and carbon management make CO₂ a promising alternative to water in geothermal systems, justifying further research and development in this area. In summary, the shift to CO₂ as a geothermal working fluid not only improves thermal performance but also promotes environmental sustainability, making it an important consideration for future geothermal energy projects⁴².

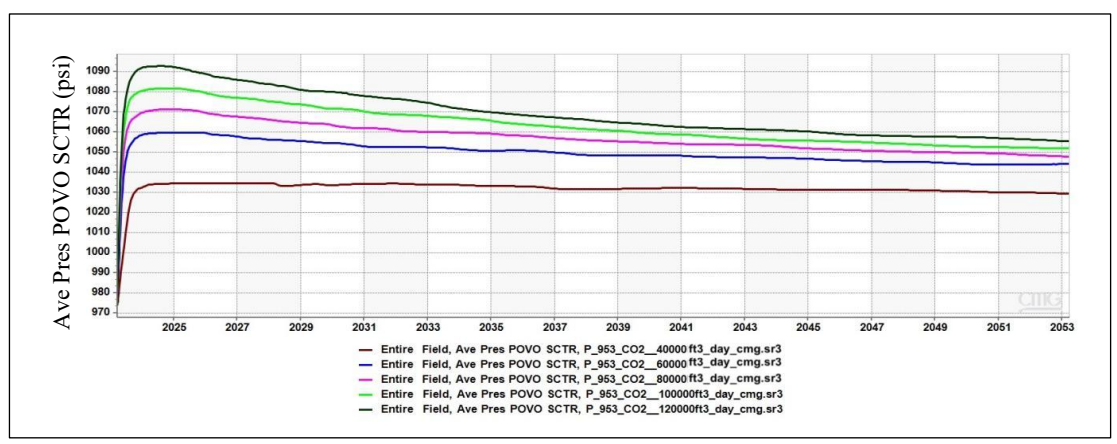


Fig. 14. Average reservoir pressure for 30 years for CO₂ injection rates (Unit psi).

Fig. 14 illustrates the simulated average reservoir pressure in the POVO sector of the field from 2025 to 2063 under varying CO₂ injection rates, ranging from 400,000 to 1,200,000 scf per day. Initially, higher injection rates result in a more rapid and elevated increase in average reservoir pressure, reflecting the capacity of CO₂ to enhance formation pressure through sustained injection. This aligns with findings from Bachu⁴⁴ and Metz et al.⁴⁵, which indicate that CO₂ injection can significantly influence reservoir pressure and aid in maintaining production by repressurising depleted reservoirs. Notably, across all injection scenarios, the average reservoir pressure of CO₂ is approximately 1055.35 psi, which plays a critical role in sustaining production. Maintaining sufficient reservoir pressure is essential in geothermal systems to drive fluid flow and support heat extraction efficiency. However, over time, despite continuous injection, all scenarios exhibit a gradual pressure decline, suggesting that reservoir depletion, fluid migration, and pressure dissipation processes eventually overcome the benefits of injection, a phenomenon also described in Zhou et al⁴⁶. The convergence of pressure values by 2053 implies diminishing marginal benefits of increasing injection rates, consistent with reservoir modelling studies which show that long-term

pressure support tends to plateau in homogeneous systems as stated by Oldenburg et al.⁴⁷. These insights support the strategic planning of CO₂-enhanced recovery and long-term storage efforts.

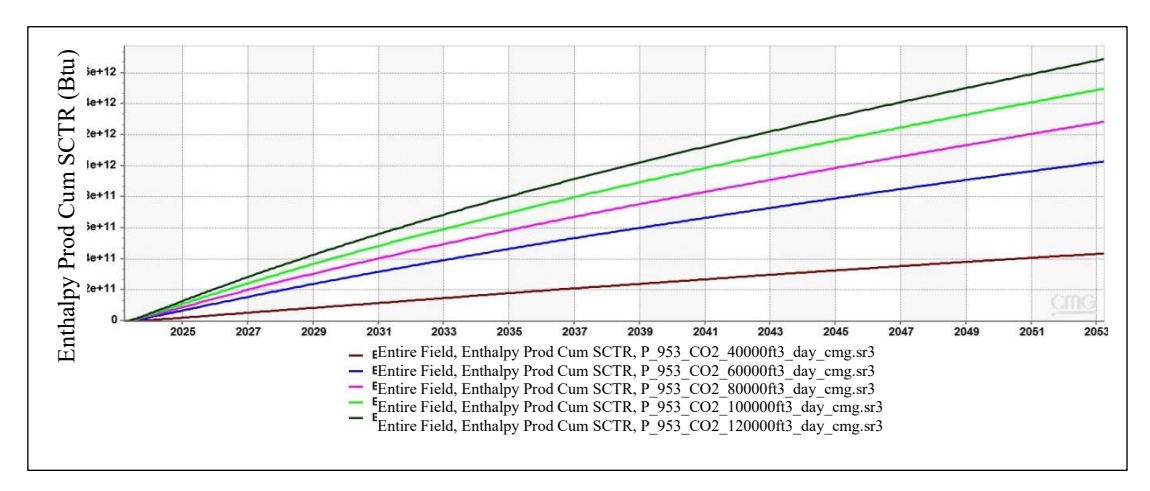


Fig. 15. Cumulative enthalpy production for 30 years for CO₂ injection rates (Unit Btu).

Fig. 15 illustrates the Enthalpy Prod Cum SCTR – Entire Field which displays the cumulative enthalpy production (in Btu) from 2025 to 2053 under five different CO₂ injection scenarios ranging from 400,000 to 1,200,000 standard cubic feet per day (scf/day). The results clearly show that higher CO₂ injection rates lead to significantly greater enthalpy recovery, with the scenario injecting 1,200,000 scf/day achieving the highest cumulative enthalpy value of approximately 1.6888 × 10¹² Btu by 2053. This trend demonstrates the strong influence of injection rate on thermal energy extraction, as greater volumes of CO₂ enhance heat transport through improved reservoir contact and sustained pressure support. Studies such as Oldenburg et al ⁴⁷ and Brown⁴⁸ have shown that using CO₂ as a working fluid in geothermal systems can increase the efficiency of heat extraction due to its low viscosity, high mobility, and ability to extract heat at a faster rate than water in certain geological settings.

Furthermore, the sharp rise in enthalpy over time with increasing injection volumes aligns with findings by Pruess.⁴⁹, who noted that CO₂'s thermophysical properties make it particularly effective for heat mining in enhanced geothermal systems (EGS), especially in low-permeability or fractured reservoirs. This makes CO₂-based geothermal systems a promising option for regions with moderate geothermal gradients, such as those hypothesized in Trinidad. The use of supercritical or near-critical CO₂ also facilitates efficient subsurface energy extraction, as emphasized by Jung et al.⁵⁰. These results underscore the potential for CO₂ to serve not only as a working fluid but also as a means of carbon sequestration, offering a dual benefit in geothermal energy systems.

Table 5 compares the thermodynamic performance of H_2O and CO_2 as working fluids in a subsurface injection system operating under a constant surface injection pressure of 1,300 psi and a bottomhole pressure of 1,000 psi, representing a pressure drop across the formation. At an injection rate of 15,000 barrels per day, water achieves an average flowing pressure of 1126.29 psi, producing an enthalpy of 5.43×10^{12} Btu and a power output of 5.45 MW. In contrast, CO_2 is injected at a higher rate of 21,360 barrels per day but with a lower average pressure of 1055.35 psi, resulting in significantly reduced enthalpy $(1.69 \times 10^{12} \text{ Btu})$ and power output (1.88 MW).

The performance difference, despite the same pressure boundaries, can be attributed to the distinct thermophysical and phase-change properties of the two fluids. Water's high specific heat capacity and enthalpy of vaporization allow it to store and transport more thermal energy per unit volume, which directly translates to higher power generation DiPippo⁵¹. CO₂, although injected at a higher volumetric rate, delivers lower thermal energy because of its lower specific enthalpy, especially under subcritical or near-critical

conditions Pruess⁴². Moreover, CO₂ tends to exhibit higher compressibility and lower density, which may result in faster fluid mobility but less efficient heat extraction per unit mass or volume Brown⁴⁸.

Under the same pressure constraints (1,300 psi at the wellhead and 1,000 psi at the bottomhole), these results reinforce that water is more effective for maximizing power output, whereas CO₂ may be better suited for applications emphasizing injectivity, pressure maintenance, and coupled geothermal—CO₂ sequestration strategies as stated by both studies Benson and Cole⁵² and Randolph and Saar⁵³. The observed average pressure values reflect how each fluid responds differently to the formation pressure gradient, influencing flow dynamics and overall system efficiency.

Table 5. Summary table for H₂O vs CO₂

Working Fluid	Injection Rate bbl/day	Average Pressure (Psi)	Enthalpy (Btu)	Power (MW)
H_2O	15000	1126.29	5.42784×10^{12}	5.4475
CO_2	21360	1055.35	1.68880×10^{12}	1.88323

5.5 Carbon dioxide reduction analysis

Table 6 shows the lowest carbon-emitting sources of electricity, producing approximately 0.18 lbs of CO₂ per kWh, mainly from minor releases of naturally occurring underground gases as stated by both US EPA⁵⁴; DiPippo⁵¹. In contrast, coal-fired power plants are the most carbon-intensive, emitting about 2.31 lbs CO₂ per kWh, primarily due to the high carbon content of coal (U.S. Energy Information Administration EIA⁵⁵. Petroleum-based generation, commonly used in diesel or oil-fired peaking plants, emits roughly 2.46 lbs CO₂ per kWh, while natural gas, considered the cleanest fossil fuel, still emits approximately 0.96 lbs CO₂ per kWh.

In TT since more than 99% of electricity produced is generated using natural gas, the amount of CO₂ which would have been emitted from 184.8 GWh of electricity would have corresponded to 393.6 million lbs. The establishment of the binary open-loop cycle geothermal power plant to replace this quantum of electricity in the grid would therefore result in CO₂ emission mitigation equivalent to that amount over the 30-year period.

Table 6. CO₂ emissions by fuel in 2021 (EIA, 2023)⁵⁵

Emissions	Geothermal	Coal	Natural Gas	Petroleum
(lbs. CO ₂ per kWh)	0.18	2.31	0.96	2.46

6 PARAMETERS FOR ECONOMICS ANALYSIS

To proceed with the economic analysis, a deterministic cashflow model is developed using a fixed annual energy supply quota of 6.2 GWh over a 30-year period along with assumed financial inputs to obtain net cashflows from the project. Firstly, the price received from the power distributor TTEC is based on US\$ 0.04 per kWh⁵⁶, which is approximately 10% below the price it currently charges to residential users (TT\$ 0.31 per kWh)⁵⁶.

According to Bruni⁵⁷ geothermal energy systems normally involve a Capital Expenditure (CAPEX) of US\$ 500,000 per MW. Given that cost savings would be achieved as no new wells would need to be drilled since existing wells in the abandoned Parryland field would be utilized, CAPEX is reduced by 50% for adoption into the cashflow model. Since the generation capacity is 0.7 MW, CAPEX is therefore estimated at US\$ 175,000. Operating expenditure (OPEX) over the 30-year investment horizon is assumed to be US\$ 0.02/kWh, which is 50% of the selling price of electricity to the distributor. Finally, to incorporate tax liabilities into the model, the corporation tax rate in TT of 30% together with a 20% capital allowance over a 5-year period is utilized.

Since cash inflows from the project are to be used to cover OPEX, CAPEX and Corporation Tax any residual would represent net cashflows. In Fig. 16, these estimated components of the cashflows model are presented. These results indicate that positive net cashflows are expected over each year of the 30-year operating lifetime of the geothermal power system.

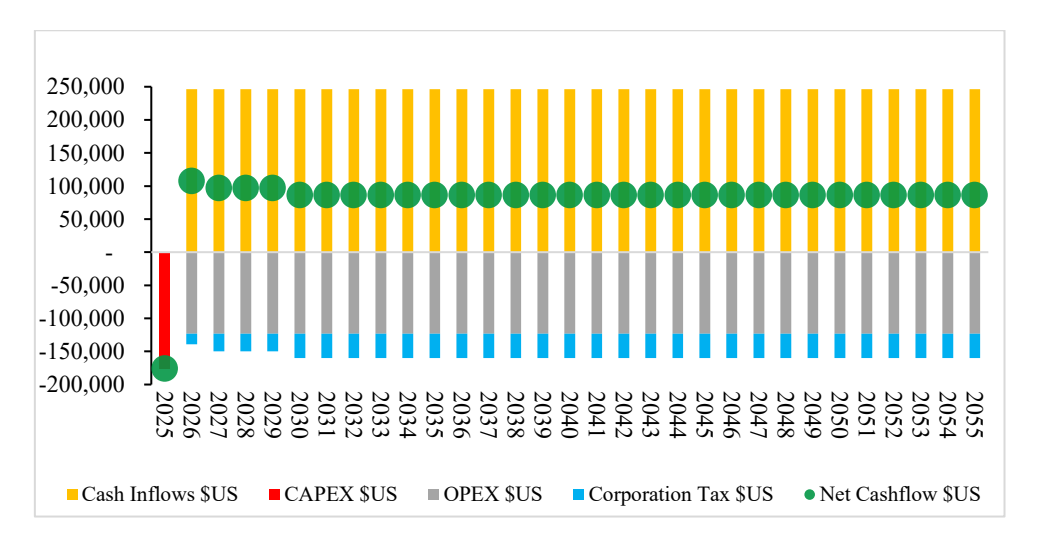


Fig. 16. Estimated cashflows from the proposed Parryland geothermal energy investment

Fig. 17 presents the distribution of the 30-year cumulative cash inflows in the form of a pie chart which highlights that net cashflows account for 33%. In addition, it must be highlighted that OPEX represents the most significant outflow at 50% compared to the other two, which consist of Corporation Tax at 14% and CAPEX at 3%. Overall, these cashflows are expected to enable a payback on the US\$175,000 investment to be achieved in the 2nd year of operations. The NPV is determined to be US\$680,000 using a minimum acceptable rate of return (MARR) of 10% and the corresponding IRR is 56%.

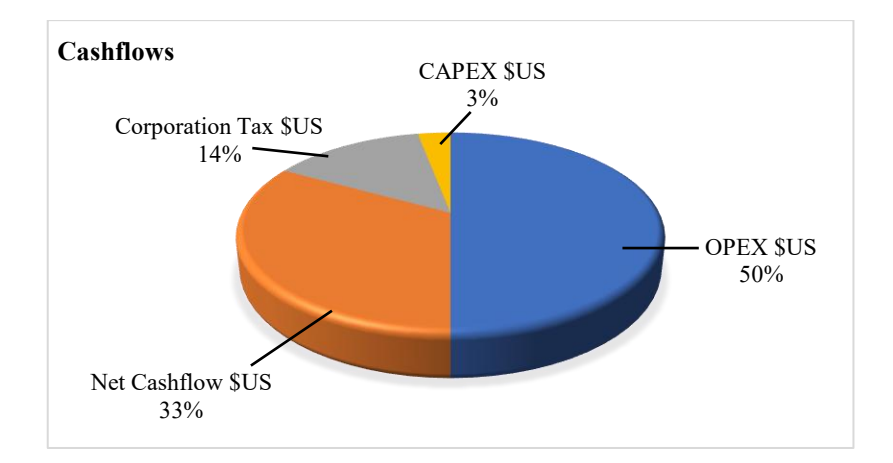


Fig. 17. Percentage distribution of cumulative cash inflows.

Monte Carlo simulations, using the Crystal Ball software, are applied to analyse how changes in assumptions affect the financial performance of the geothermal power plant investment. This involves subjecting the deterministic economic model to variations in its input assumptions. This procedure involves

using probability distributions for the core variables, listed in Table 7, where the uniform probability distribution is assumed for each. Under this type of distribution, a continuous range of possible values defined by a minimum and maximum inclusive are assigned to the variable with each individual value having an equal probability of occurrence.

Table 7. Assumed probability distributions of key variables in the economic models

Variable	Base Case	Probability Distribution	Minimum	Maximum
Electricity Price (US\$/kWh)	0.04	Uniform	0.035	0.045
Efficiency (%)	12%	Uniform	12%	21%
CAPEX (US\$/MW)	500,000	Uniform	500,000	1,000,000
OPEX (US\$/kWh)	0.02	Uniform	0.01	0.03

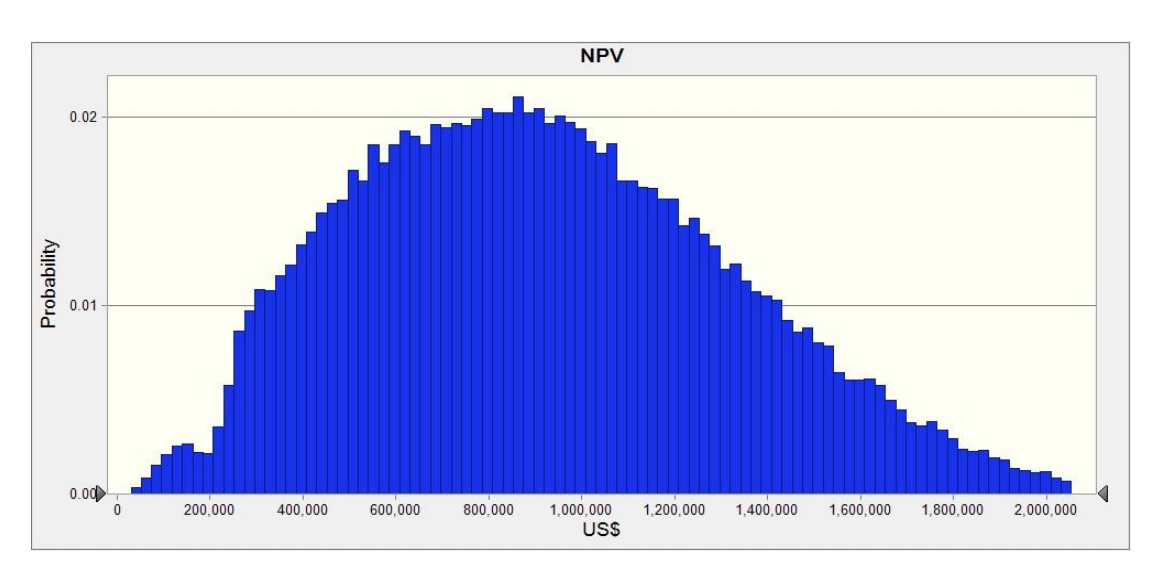


Fig. 18. Forecast chart of NPV based on Monte Carlo Simulations.

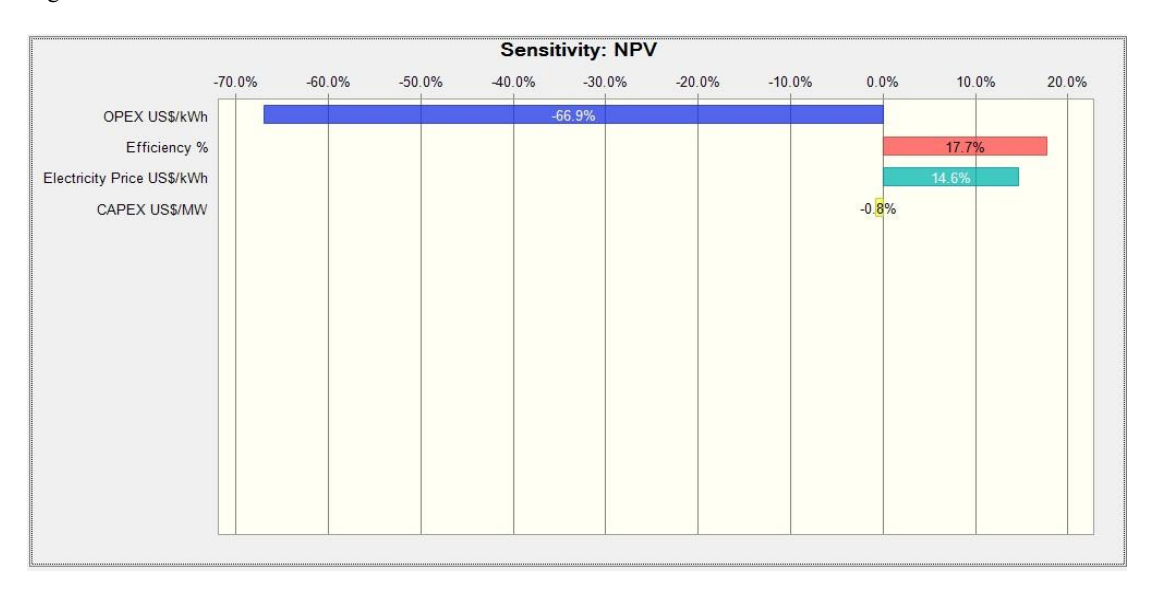


Fig. 19. Sensitivity analysis of NPV under Monte Carlo Simulations.

https://doi.org/10.24191/jsst.v5i2.110

The Crystal ball software changed each of these inputs in the economic model by choosing random values within the specification of the assumed probability distribution and recalculated the NPV over a selection of 1,000,000 trials. This resulting possibility space of 1,000,000 NPVs and the associated probabilities arising from the combined independent probabilities of each combination of randomly selected input variables is presented in the graphical form in Fig. 18. This shows that the NPV is not expected to become negative, which implies there is 100% certainty that the return on the investment is projected to exceed the MARR, should the input variables change within the assumed minimum and maximum intervals specified in Table 7. Furthermore, the rightward skew of the NPV forecast indicates a wider range of upside potential on earnings, significantly higher levels of NPV compared to those in the original deterministic cashflow model.

A sensitivity analysis is performed within the Monte Carlo Simulations as presented in graphical form in Fig. 19 This highlights that the most significant economic input which influences the performance of the investment in the geothermal plant is OPEX, the ramifications of which are that this variable must be carefully managed to maintain the feasibility of the long-term renewable energy project.

7 CONCLUSIONS

This study examined the technical and economic outcomes of retrofitting the defunct Parryland oil field with a geothermal power plant to harness thermal energy to generate clean electricity. It compiled and synthesised existing research and global projects to highlight the opportunities and challenges associated with developing geothermal energy through the repurposing of hydrocarbon wells. The reservoir had an average sand thickness of 75 feet, shale depths ranging from 10 to 17.5 feet and an assumed temperature of 212 °F, which resulted in an optimal geothermal system configuration based on 3 injectors and 3 producer wells spaced at 900 feet with water injection of 15,000 barrels per day at 1,300 psi. The calculated cumulative enthalpy from the reservoir over a 30-year period was 5.385 trillion Btu, of which 5.254 trillion Btu of usable heat could be converted to 184.8 GWh of electricity, which is expected to mitigate 157.1 million lbs of CO₂ emissions. The capacity of the geothermal plant was estimated at 0.7MW which is envisaged to cost half the typical CAPEX of such investments due to the utilization of existing well infrastructure in the abandoned Parryland oil field.

Overall, the investment is economically feasible with a relatively short payback of 2 years, an NPV of US\$680,000 and an estimated IRR of 56%. The sensitivity analysis of the financial performance of the geothermal power plant indicates that there is 100% certainty that a positive return on the investment would be realised. The proposed project is, therefore, an innovative and economically sustainable means of implementing a renewable energy initiative, made more cost-effective by repurposing existing infrastructure in a depleted hydrocarbon reservoir. In addition, the retrofitted geothermal power plant holds immense significance for TT and the wider region as its implementation would mark the first instance of a retrofitted geothermal system in this geographical area, signalling a significant advancement in sustainable energy practices. This initiative also has the potential to create new job opportunities while also adhering to the Paris accord ratified by the Government of TT in 2018.

ACKNOWLEDGEMENTS/ FUNDING

The authors would like to acknowledge the support of both Dr. David Alexander and Dr. Edward Bahaw for their assistance in the preparation of this manuscript according to the required format. There was no funding received for this research.

CONFLICT OF INTEREST

The authors agree that this research was conducted in the absence of any self-benefits, commercial or financial conflicts and declare the absence of conflicting interests with the funders.

AUTHORS' CONTRIBUTIONS

Conceptualization: D. Alexander

Data curation: M. Ragoobar, D. Alexander, E. Bahaw

Methodology: M. Ragoobar, D. Alexander

Formal analysis: M. Ragoobar Visualisation: Not Applicable

Software: Computer Modelling Group (CMG), Oracle Crystal Ball

Writing (original draft): M. Ragoobar

Writing (review and editing): D. Alexander, E. Bahaw

Validation: D. Alexander, E. Bahaw Supervision: D. Alexander, E. Bahaw E. Funding acquisition: Not Applicable Project administration: M. Ragoobar

REFERENCES

- 1. Nkinyam, C. M., Ujah, C. O., Asadu, C. O., & Kallon, D. V. V. (2025). Exploring geothermal energy as a sustainable source of energy: A systemic review. *Unconventional Resources*, 6, 100149. https://doi.org/10.1016/j.uncres.2025.100149
- 2. Nian, Y.-L., & Cheng, W.-L. (2018). Evaluation of geothermal heating from abandoned oil wells. *Energy*, 142, 592–607 | 10.1016. https://doi.org/10.1016/j.energy.2017.10.062
- 3. Nicholson, K. (1993). Geothermal fluids. Springer. https://doi.org/10.1007/978-3-642-77844-5
- 4. Schütz, F., Winterleitner, G., & Huenges, E. (2018). Geothermal exploration in a sedimentary basin: New continuous temperature data and physical rock properties from northern Oman. *Geothermal Energy*, 6(1), Article 11. https://doi.org/10.1186/s40517-018-0091-6
- 5. Keane, C. (2020). What is an Enhanced Geothermal System? *American Geoscience Institute* https://profession.americangeosciences.org/society/intersections/faq/enhanced-geothermal-system/
- 6. U.S. Energy Information Administration (2022). *Geothermal explained: Geothermal energy and the environment.* https://www.eia.gov/energyexplained/geothermal/geothermal-energy-and-the environment.php
- 7. Mehmood, A., Yao, J., Fan, D., Bongole, K., Liu, J., & Zhang, X. (2019). Potential for heat production by retrofitting abandoned gas wells into geothermal wells. *PLOS ONE*, *14*(8), e0220128. https://doi.org/10.1371/journal.pone.0220128
- 8. Ritchie, H., Rosado, P., & Roser, M. (2023). *CO₂ and greenhouse gas emissions. Our World in Data.* https://ourworldindata.org/co2-and-greenhouse-gas-emissions
- 9. Doman, L. (2017, January 5). *EIA projects 28% increase in world energy use by 2040*. U.S. Energy Information Administration. https://www.eia.gov/todayinenergy/detail.php?id=32912
- 10. Ministry of Planning and Development. (2016). Vision 2030: The national development strategy of Trinidad and Tobago 2016–2030. Government of Trinidad and Tobago. https://www.planning.gov.tt/sites/default/files/Vision%202030%20The%20National%20Developme nt%20Strategy%20of%20Trinidad%20and%20Tobago%202016-2030.pdf
- 11. CEIC (n.d). *Trinidad and Tobago crude oil production*. https://www.ceicdata.com/en/indicator/trinidad-and-tobago/crude-oil-production

- 12. Indar. D. (2019). *National energy efficiency monitoring report of Trinidad and Tobago*. United Nations Economic Commission for Latin America and the Caribbean (ECLAC). https://ideas.repec.org/p/ecr/col022/45051.html
- 13. Sun, Y., Sun, M., & Tang, X. (2019). Influence analysis of renewable energy on crude oil future market. *In 2019 IEEE 3rd International Conference on Green Energy and Applications (ICGEA)*, 167-171. IEEE. https://doi.org/10.1109/ICGEA.2019.8880778
- 14. United Nations Framework Convention on Climate Change (UNFCCC). (2015). Key aspects of the Paris Agreement. https://unfccc.int/most-requested/key-aspects-of-the-paris-agreement
- 15. Ministry of Energy and Energy Affairs (2011). Framework for development of a renewable energy policy for Trinidad and Tobago a report of the renewable energy committee. https://www.energy.gov.tt/wp-content/uploads/2014/01/Framework-for-the-development-of-arenewable-energy-policy-for-TT-January-2011.pdf
- 16. Jello, J., & Baser, T. (2023). Utilization of existing hydrocarbon wells for geothermal system development: A review. *Applied Energy*, 348, 121456. https://doi.org/10.1016/j.apenergy.2023.121456
- 17. Tester, J. W., Herzog, H. J., Chen, Z., Potter, R. M., & Frank, M. G. (1994). Prospects for universal geothermal energy from heat mining. *Science & Global Security*, 5(1), 99-121. https://doi.org/10.1080/08929889408426418
- 18. Toth, A. N., Szucs, P., Pap, J., Nyikos, A., & Fenerty, D. K. (2018). *Converting abandoned Hungarian oil and gas wells into geothermal sources* (SGP-TR-213). In *Proceedings of the 43rd Workshop on Geothermal Reservoir Engineering* (pp. 1–8). Stanford University. Retrieved from https://pangea.stanford.edu/ERE/pdf/IGAstandard/SGW/2018/Toth.pdf.
- 19. International Energy Agency (2024). *The future of geothermal energy*. International Energy Agency. https://www.iea.org/reports/the-future-of-geothermal-energy
- 20. International Renewable Energy Agency (2024). Renewable power generation costs in 2023. https://www.irena.org/-/media/Files/IRENA/Agency/Publication/2024/Sep/IRENA_Renewable _power_generation_costs_in_2023.pdf
- 21. TWI Global. (2025). What are the advantages and disadvantages of geothermal energy? https://www.twi-global.com/technical-knowledge/faqs/geothermal-energy/pros-andcons# What are the Disadvantages of Geothermal Energy
- 22. Kurnia, J. C., Shatri, M. S., Putra, Z. A., Zaini, J., Caesarendra, W., & Sasmito, A. P. (2022). Geothermal energy extraction using abandoned oil and gas wells: Techno-economic and policy review. *International Journal of Energy Research*, 46(1) 28-60. https://doi.org/10.1002/er.6386
- 23. Maurel, C., Hamm, V., Bugarel, F., & Maragna, C. (2020). *Inventory and first assessment of oil and gas wells conversion for geothermal heat recovery in France* [Conference paper]. HAL Open science / BRGM. https://brgm.hal.science/hal-02306770/document
- 24. Deville, E., & Guerlais, S.-H. (2009). Cyclic activity of mud volcanoes: Evidences from Trinidad (SE Caribbean). *Marine and Petroleum Geology*, 26(9), 1681–1691. https://doi.org/10.1016/j.marpetgeo.2009.03.002
- 25. Dickson, M. H., & Fanelli, M. (2013). *Geothermal energy: utilization and technology* (1st ed.). Routledge. https://doi.org/10.4324/9781315065786

- 26. Bell-Eversley, J., Ramnath, C., Alexander, D., Maharaj, R., & Boodlal, D. (2022). The Potential of Utilizing Geothermal Energy Coupled with Geomechanics: A case Study for Trinidad and Tobago. *International Journal of Renewable Energy Research*, 12(1), 305–319. https://doi.org/10.20508/ijrer.v12i1.12795.g8406
- 27. Patihk, J., Warner-Lall, D., David, D., Maharaj, R., & Boodlal, D. (2021). The optimization of a potential geothermal reservoir using abandoned wells: A case study for the forest reserve field in Trinidad, *Journal of Petroleum Exploration and Production Technology*, 12(1), 239–255. https://doi.org/10.1007/s13202-021-01322-y
- 28. Bloomfield, K., & Moore, J. (1999). Geothermal electrical production CO₂ emissions study. Geothermal Resource Council 1999 Annual Meeting. https://inldigitallibrary.inl.gov/sites/sti/3314491.pdf
- 29. Ramlal, V. (2004). Enhanced oil recovery by steamflooding in a recent steamflood project, Cruse "E" Field, Trinidad. *SPE/DOE Symposium on Improved Oil Recovery*. (pp. 17–21) https://doi.org/10.2118/89411-ms
- 30. Liang, B., Jiang, H., Li, J., & Gong, C. (2015). A systematic study of fracture parameters effect on fracture network permeability based on discrete-fracture model employing Finite Element Analyses. *Journal of Natural Gas Science and Engineering*, 28, 711–722. https://doi.org/10.1016/j.jngse.2015.12.011
- 31. Zhu, G., Yao, J., Sun, H., Zhang, M., Xie, M., Sun, Z., & Lu, T. (2015). The numerical simulation of thermal recovery based on hydraulic fracture heating technology in shale gas reservoir. *Journal of Natural Gas Science and Engineering*, 28, 305–316. https://doi.org/10.1016/j.jngse.2015.11.051
- 32. Zhang, Q., Huang, Z., Yao, J., Wang, Y., & Li, Y. (2017). Multiscale mimetic method for two-phase flow in fractured media using embedded discrete fracture model. *Advances in Water Resources*, 107, 180–190. https://doi.org/10.1016/j.advwatres.2017.06.020
- 33. Xu, C., Dowd, P. A., & Tian, Z. F. (2014). A simplified coupled hydro-thermal model for enhanced geothermal systems. *Applied Energy*, *140*, 135–145. https://doi.org/10.1016/j.apenergy.2014.11.050
- 34. Fofinha, L. (2019). IRENA Geothermal Power *Wayne*. https://www.academia.edu/39447889/IRENA Geothermal Power
- 35. U.S. Environmental Protection Agency (2023). *Greenhouse gas inventory guidance direct emissions from stationary combustion sources*. https://www.epa.gov/sites/default/files/2020-12/documents/stationaryemissions.pdf
- 36. Boodlal, D., Alexander, D., & Narinesingh, J. (2014). The use of reservoir simulation to obtain key parameters for investigating the feasibility of implementing flue gas CO₂-EOR coupled with sequestration in Trinidad. *Energy Procedia*, 63, 7517–7528. https://doi.org/10.1016/j.egypro.2014.11.788
- 37. Doghaish, N. M. (2008). *Analysis of enhanced oil recovery processes A literature review* (Master's thesis, Dalhousie University, Canada. https://central.bac-lac.gc.ca/.item?id=MR50008&op=pdf&app=Library&oclc_number=710885058
- 38. Zarrouk, S. J., & Moon, H. (2014). Efficiency of geothermal power plants: A worldwide review. *Geothermics*, 51, 142–153. https://doi.org/10.1016/j.geothermics.2013.11.001
- 39. Quaschning, V. (2005). *Understanding renewable energy systems*. Routledge, https://www.cleanenergo.ru/wp-content/uploads/files/knigi/solar_energ/understanding-renewable-energy-systems.pdf

- 40. U.S. Department of Energy (2004). *Geothermal technologies program: Buried treasure*. https://www.nrel.gov/docs/fy05osti/35939.pdf
- 41. Liu, H., Li, Q., Gou, Y., Zhang, L., Feng, W., Liao, J., Zhu, Z., Wang, H., & Zhou, L. (2020). Numerical modelling of the cooling effect in geothermal reservoirs induced by injection of CO₂ and cooled geothermal water. *Oil & Gas Science and Technology Revue d'IFP Energies Nouvelles*, 75, 15. https://doi.org/10.2516/ogst/2020005
- 42. Pruess, K. (2008). On production behavior of enhanced geothermal systems with CO₂ as working fluid. *Energy Conversion and Management*, 49(6), 1446-1454. https://doi.org/10.1016/j.enconman.2007.12.029
- 43. Liu, Y., Wang, G., Yue, G., Zhang, W., Zhu, X., & Zhang, Q. (2018). Comparison of enhanced geothermal system with water and CO₂ as working fluid: A case study in Zhacanggou, Northeastern Tibet, China. *Energy Exploration & Exploitation*, 37(2), 736–755. https://doi.org/10.1177/0144598718795492
- 44. Bachu, S. (2003). Screening and ranking of sedimentary basins for sequestration of CO₂ in geological media. *Environmental Geology*, 44(3), 277–289. https://doi.org/10.1007/s00254-003-0762-9
- 45. Metz, B., Davidson, O., De Coninck, H. C., Loos, M., & Meyer, L. (2005). *IPCC Special report on carbon dioxide capture and storage*. Cambridge: Cambridge University Press.
- 46. Zhou, Q., Birkholzer, J.T., Tsang, C.-F., & Rutqvist, J. (2008). A method for quick assessment of CO₂ storage capacity in closed and semi-closed saline formations. *International Journal of Greenhouse Gas Control*, 2(4), 626–639. https://doi.org/10.1016/j.ijggc.2008.02.004
- 47. Oldenburg, C. M., Moridis, G. J., Spycher, N., & Pruess, K. (2004). EOS7C version 1.0: TOUGH2 module for carbon dioxide or nitrogen in natural gas (methane) reservoirs. .Lawrence Berkeley National Laboratory
- 48. Brown, D. W. (2000). A hot dry rock geothermal energy concept utilizing supercritical CO₂ instead of water. In *Proceedings of the 25th Workshop on Geothermal Reservoir Engineering (2000)*, Stanford University.
- 49. Pruess, K. (2006). Enhanced Geothermal Systems (EGS) Using CO₂ as Working Fluid A Novel Approach for Generating Renewable Energy with Simultaneous Sequestration of Carbon. Geothermics, 35(4), 351–367. doi:10.1016/j.geothermics.2006.08.002.
- 50. Jung, R., Kohl, T., & Rummel, F. (2014). Hydraulic stimulation and reservoir development. In *Geothermal Energy Systems* (pp. 63–92). Wiley. Did not find the validity of reference
- 51. DiPippo, R. (2016). Geothermal power plants: Principles, applications, case studies and environmental impact. Butterworth-Heinemann.
- 52. Benson, S. M., & Cole, D. R. (2008). CO₂ sequestration in deep sedimentary formations. *Elements*, 4(5), 325–331.https://doi.org/10.2113/gselements.4.5.325
- 53. Randolph, J. B., & Saar, M. O. (2011). Combining geothermal energy capture with geologic carbon dioxide sequestration. *Geophysical Research Letters*, 38(10). https://doi.org/10.1029/2011gl047265
- 54. U.S. Environmental Protection Agency (EPA). (2023). *Greenhouse Gas Emissions from the Power Sector*. www.epa.gov
- 55. U.S Energy Information Administration (2023). How much carbon dioxide is produced per kilowatthour of US electricity generation? https://www.eia.gov/tools/faqs/faq.php?id=74&t=11

- 56. Trinidad and Tobago Electricity Commission (2024). Tariffs Trinidad and Tobago Electricity Commission. https://ttec.co.tt/tariffs-2
- 57. Bruni, S. (2015). Three steps to ensure that geothermal energy takes off Sostenibilidad. Inter-American Development Bank. https://blogs.iadb.org/sostenibilidad/en/three-steps-ensure-geothermal-energy-takes/